Effect of electrode materials on the photo-electric response of a hybrid solar cell-supercapacitor with a photoactive gel electrolyte

Reza Amirabad, Arash Takshi

Reza Amirabad, Arash Takshi, "Effect of electrode materials on the photo-electric response of a hybrid solar cell-supercapacitor with a photoactive gel electrolyte," Proc. SPIE 12668, New Concepts in Solar and Thermal Radiation Conversion V, 1266806 (26 September 2023); doi: 10.1117/12.2676938

SPIE.

Event: SPIE Optical Engineering + Applications, 2023, San Diego, California, United States

Effect of electrode materials on the photo-electric response of a hybrid solar cell-supercapacitor with a photoactive gel electrolyte

Reza Amirabad[a] and Arash Takshi[*a]
[a] Department of Electrical Engineering, University of South Florida, Tampa FL, U.S.A.

ABSTRACT

Due to the increasing demand for using compact and low-power wireless sensors, the interest in designing hybrid cells with the dual properties of energy harvesting and storage has been growing in recent years. Among different designs, two-electrode hybrid cells are more suitable for low-voltage and low-power electronics. Using a redox-active polyvinyl alcohol (PVA)/polyaniline (PANI)-based gel electrolyte, a two-terminal device was fabricated and tested in this study. The performance of the gel electrolyte was assessed in different devices made from a carbon nanotube-based cathode and four different anodes. All the tested anodes were made from a conductive glass coated with mesoporous TiO_2, transparent TiO_2, opaque TiO2, or mesoporous ZrO_2. Cyclic voltammetry (CV), open circuit voltage (OCV), and short circuit current (SCC) were conducted to investigate the properties of the devices. The fabricated device with the transparent TiO_2 coating has shown a capacitance of 0.363 mF and with the opaque TiO_2 coating has shown a photovoltaic potential of 244 mV. The results suggest further studies on materials nanostructure to achieve higher energy conversion efficiency and larger storage capacitances for future applications in wireless devices.

Keywords: Hybrid solar cell-supercapacitor, Anode material, Poly aniline, Polyvinyl alcohol.

1. INTRODUCTION

Given the rapid proliferation of wireless sensors, a subset of devices has emerged that leverages ambient light and solar energy as viable power sources for their circuits [1, 2]. One of the prevailing challenges encountered when employing solar cells to energize electronic devices lies in the inherent intermittency of this energy source. Solar energy can solely be harnessed during daylight hours, and its effectiveness is contingent upon prevailing weather conditions. Consequently, it becomes imperative to meticulously engineer a system that encompasses adequate output power and storage capacity to ensure a steadfast and uninterrupted supply of electrical power [3].

Typically, a solar energy system incorporates an external battery or supercapacitor. However, the physical dimensions of both the solar cell and storage unit tend to be excessively large for compact wireless sensors. Consequently, in recent years, numerous research teams have endeavored to develop hybrid cells that possess the dual capabilities of solar energy harvesting and storage. It has been demonstrated that a diverse array of innovative approaches can be employed to address the objective of creating hybrid cells, ranging from straightforward integration of two devices within a single package to novel architectures utilizing emerging materials [4]. In general, devices that integrate a solar cell and a storage unit in a unified package necessitate the incorporation of a switching mechanism between the two cells [5].

Nonetheless, the studies conducted thus far have overlooked the concept of energy storage. Previously, our research group developed photoactive supercapacitors utilizing a conducting polymer (CP) photoanode [6]. Although this device exhibited a respectable storage capacitance, its photovoltaic performance was constrained by the thin CP layer. Consequently, the design of the hybrid cell was modified to integrate the CP within the electrolyte, enabling the bulk of the electrolyte to serve as a medium for light absorption and charge storage [7]. In this new design, a composite gel electrolyte composed of polyvinyl alcohol (PVA) and polyaniline (PANI) was synthesized and employed between two electrodes [8]. The operational mechanism relies on the PANI within the bulk gel absorbing light and generating positive and negative electronic and ionic charges, respectively. By utilizing distinct electrodes, charges can be separated to generate a photocurrent. However, in scenarios where the output current is lower than the rate of charge generation (such as the open circuit mode), the photo-generated charges can be stored within the system by altering the oxidation state of PANI. While our earlier investigations demonstrated the feasibility of utilizing the composite gel to fabricate planar and fiber-shaped

New Concepts in Solar and Thermal Radiation Conversion V, edited by
Peter Bermel, Jeremy N. Munday, Proc. of SPIE Vol. 12668, 1266806
 · 0277-786X · doi: 10.1117/12.2676938

hybrid devices [9], further research is warranted to comprehend the impact of constituent materials and their concentrations on the photoelectric properties of the gel electrolyte. This research endeavor primarily centered on anode material. Within this study, we investigated the utilization of various types of anode electrodes, aiming to assess the influence of different anodes on the performance of the devices. Specifically, we examined four distinct anodes, namely: glass coated with mesoporous TiO_2, Ti-Nanoxide, Ti-Nanoxide coated with a reflective layer, and mesoporous ZrO_2.

2. METHODOLOGY

2.1 Materials and Equipment

Solaronix provided the fluorine tin oxide (FTO) electrode coated with mesoporous TiO_2 (highly transparent, 15-20 nm anatase particles), transparent TiO_2 (highly dispersed, very high surface area), opaque TiO_2 (optimal mixing of large and small nanoparticles ensures both very high surface area and light diffusion), or mesoporous ZrO_2. The main differences between titania electrodes lie in their transparency (opaque or transparent) and structure (mesoporous or non-mesoporous). Opaque electrodes maximize light absorption, while transparent electrodes prioritize light transmission. Mesostructured titania electrodes offer enhanced performance due to their large surface area and improved charge transport characteristics. The ZrO2 electrode has indeed a multilayer structure of compact titania and mesoporous titania on FTO with a thin mesoporous ZrO_2 on top of all with the overall thickness of coatings to be ~1 μm. All other chemicals and materials, including multi-walled carbon nanotubes (MWCNTs), polyvinyl alcohol (PVA), phosphoric acid (H_3PO_4), aniline, and ammonium persulfate (APS), were obtained from Sigma-Aldrich.

2.2 Preparation of carbon nanotube electrode

In this research, the porous carbon nanotube electrode was created using the method described in our earlier works [10]. To prepare the conductive ink solution, a mixture consisting of 30 milliliters of deionized (DI) water, 300 milligrams of carbon nanotubes (CNTs), and 150 milligrams of sodium dodecylbenzenesulfonate (SDBS) was sonicated at room temperature for 30 minutes. Subsequently, 1 milliliter of this solution was drop-casted onto a 4.0 cm × 7.0 cm piece of paper, which was then dried in a vacuum oven at 120 °C for 30 minutes. This process was repeated three times to ensure the production of suitable electrodes. The papers coated with conductive ink were then cut into 4 cm × 1 cm pieces with a thickness of 150 μm. The electrical conductivity of the carbon nanotube electrodes was measured to be 98 $S.cm^{-1}$ using a 4-probe Keithley (2602) instrument.

2.3 Preparation of PVA/PANI hydrogel

In this research, we created four different supercapacitor and solar hybrid cells with varying working electrodes including mesoporous ZrO_2 and mesoporous, Transparent, and Opaque TiO_2. To achieve this, we first dissolved 5 grams of PVA in 100 milliliters of 1 M phosphoric acid at a temperature of 80 °C over a period of 6 hours. Subsequently, we prepared solutions of APS 0.1 M in 1 M phosphoric acid at room temperature, which were then added to the PVA solution. Finally, we slowly introduced 3 milliliters of aniline to initiate in-situ polymerization, and the resulting gel was mixed at room temperature for 12 hours.

2.4 Device fabrication and characterization

The composite gel was applied as a coating on both the anode and CNT electrodes. To separate the two electrodes, three layers of fiberglass mesh with a thickness of around 710 μm were utilized. The electrodes were placed between two glass plates and secured together using paper clips. Copper tape was employed to establish contact for measurement purposes. Figure 1 has shown a schematic of the structure and a picture of a fabricated device.

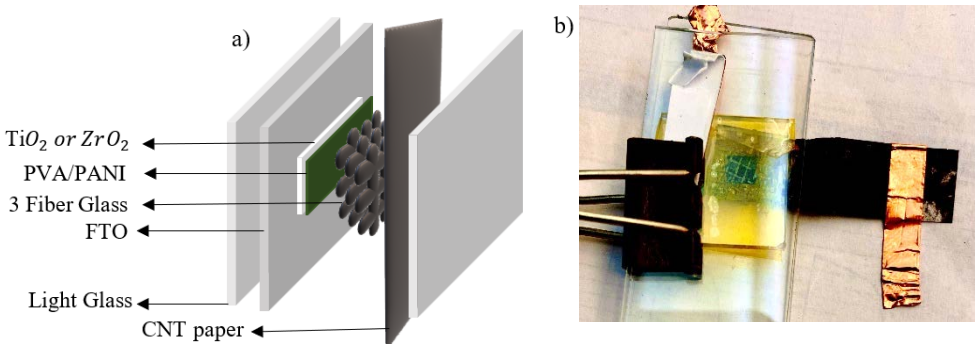

Figure 1. a) a schematic of the structure and b) a picture of a fabricated device.

The electrochemical and electrical evaluations, including Cyclic Voltammetry (CV), Chronopotentiometry (CP), Electrochemical Impedance Spectroscopy (EIS), open circuit voltage (OC), and short circuit current (SC), were measured using a VersaSTAT 4 potentiostat with a two-terminal configuration. CVs were performed at a scan rate of 50 mV/s. This paper presents the third cycle of each experiment, which was repeated five times. The EIS investigations covered a frequency range from 0.1 Hz to 10 kHz, with an AC voltage amplitude of 20 mV at 0.0 V DC bias. CV, CP, and EIS tests were conducted in a dark environment, while OC and SC measurements were carried out using a solar light simulator, specifically the Radiant Source Technology (RST), with an output power intensity of 80 $mW.cm^{-2}$. The solar simulator was equipped with an internal AM 1.0 optical filter to ensure the light spectrum resembled that of standard sunlight. However, all analyses were conducted at room temperature.

3. RESULTS and DISCUSSION

At first, to determine the capacitance of each device, CV experiments were performed. CV analysis was conducted by applying a potential range of -0.5 V to +0.5 V and utilizing a scan rate of 50 mV/s. To eliminate the influence of ambient light, the CV measurements were conducted in a light-free enclosure. Based on the width of the loop (Figure 2.a), it was evident that the highest capacitance was from the device with the transparent TiO_2 and the lowest was from the device with the mesoporous ZrO_2 electrode. However, after one week, there was a remarkable change in CV results. As shown in Figure 2.b, the capacitance was enhanced noticeably in the device with the mesoporous ZrO_2 electrode. Also, redox peaks appeared in the same device. There are peaks as a result.

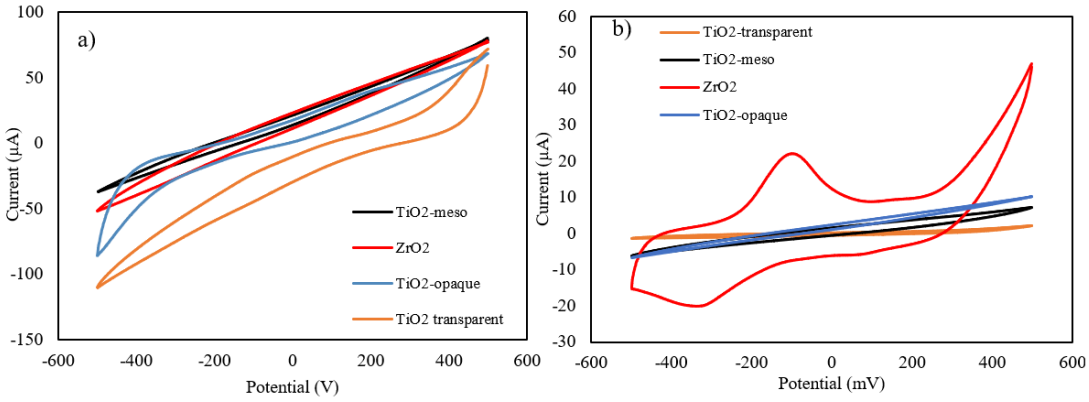

Figure 2: Cyclic voltammetry results of the hybrid device with different anodes were made from a conductive glass coated with mesoporous TiO_2, transparent TiO_2, opaque TiO_2, or mesoporous ZrO_2 at a) first day and b) after one week.

The determination of capacitance involves studying the response of the device as the current, I, undergoes variations. In cyclic voltammetry (CV) experiments, the current changes in response to the voltage across the two terminals. Thus, the capacitance, C, can be expressed as follows [11-13]:

$$C = \frac{\int IdV}{\Delta V . S} \qquad (1)$$

where ΔV represents the difference between the initial and final potentials, S denotes the voltage scan rate, and $\int IdV$ corresponds to the area under the CV curve. Using Equation 1, the capacitance of the devices was estimated and reported in Table 1. While the capacitance of the transparent and opaque electrodes was significantly higher than the other two on day 1, the device with ZrO_2 showed a significant improvement after one week. At the same time, all three devices showed a substantial decrease in capacitance. The results suggest that when the device was fresh, the gel electrolyte easily diffused into the high surface area of the transparent and opaque TiO_2, but perhaps the ZrO_2 layer had limited the interface of the gel with the underlying compact titania and mesoporous titania layers. After a week, the gel had been diffused into the 1 µm thick multilayer-porous structure. More importantly, it is evident that the ZrO_2 layer was protecting the TiO_2 layers resulting in a high stability after one week. Also, the redox peaks imply the unique nature of the interface between ZrO_2 and the gel.

Table.1: The characteristics of devices.

Cells with different anodes	First day Capacitance (mF)	First week Capacitance (mF)
Transparent TiO_2	0.363	0.0122
Mesoporous TiO_2	0.099	0.03
Mesoporous ZrO_2	0.18	0.336
Opaque TiO_2	0.334	0.018

The galvanostatic charge-discharge profiles of the hybrid devices were investigated using the chrono-potentiometry (CP) method, employing constant currents of ±50 µA. This analysis aimed to comprehend the impact of varying the anode electrodes on the series resistance (*Rs*). As a result of the faradaic reaction, the charge-discharge curves exhibited non-linear characteristics during the charging and discharging cycles, as depicted in Figure 3a and b [14]. Additionally, Table 2 illustrates that voltage drop (ΔV_R) at the transition between the charging and discharging cycles for the four devices when they were fresh and one week after the fabrication. It should be noted that since the charging and discharging currents were switched between of +50 µA and of -50 µA, the magnitude of ΔV_R is directly proportional to the series resistance, *Rs*, of the cells (ΔV_R= *Rs* x100 µA).

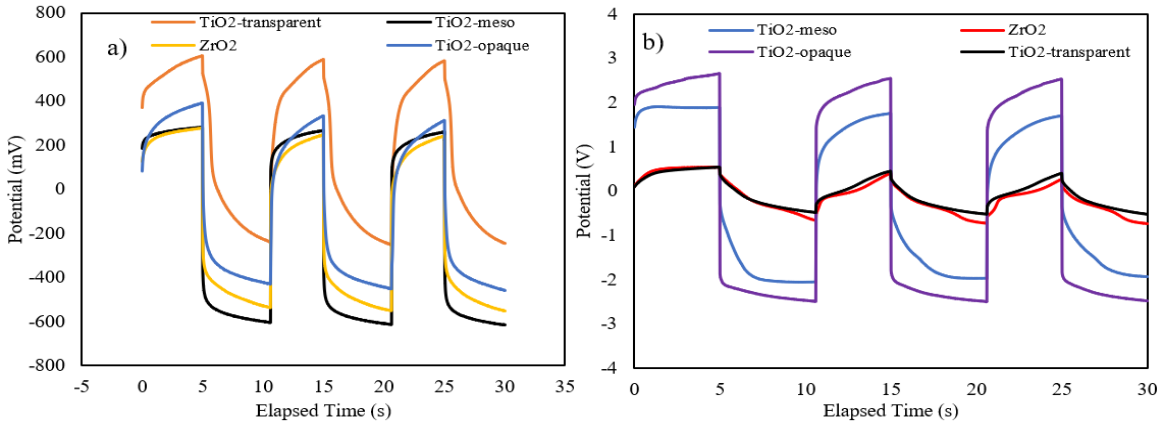

Figure 3: The CP experiments of hybrid devices with different anodes a) first day and b) after one week.

Table.2: The voltage drop (ΔV_R).

Cells with different anodes	First day ΔV_R(V)	First week ΔV_R(V)
Transparent TiO_2	0.065	0.197
Mesoporous TiO_2	0.728	2.231
Mesoporous ZrO_2	0.5496	0.179
Opaque TiO_2	0.524	4.410

The numerical results in Table 2 show the low resistance of the transparent titania on day one that was increased by three folds after one week. Other TiO_2 electrodes also showed an increase in *Rs* after a week, but the protective ZrO_2 actually reduced *Rs*.

To achieve optimal performance, it is imperative to consider the photovoltaic effect of the devices, even as the energy storage performance remains significant in hybrid cells. Consequently, the photovoltaic performance of the device was evaluated utilizing established techniques commonly employed for assessing the performance of dye-sensitized solar cells (DSSCs). This evaluation was conducted due to the capability of the PVA/PANI gel electrolyte to absorb light and function as an active layer, as demonstrated in Figure 4. To investigate the photovoltaic effect of the hybrid device with varying anode electrode, an open circuit (OC) measurement was performed in two stages. Firstly, the hybrid device was subjected to illumination for 650 seconds, followed by a subsequent dark period of 350 seconds, as depicted in Figure 4. As expected from the capacitance results, when the device with the ZrO_2 electrode was fresh, no photovoltaic activity was observed, but after one week the photovoltaic voltage (voltage difference between dark and light) reached to 90 mV. This parameter was 81 mV in the opaque TiO_2. However, the highest magnitude of the open circuit voltage was from the opaque TiO_2 ($|V_{oc}|$=0.244 V).

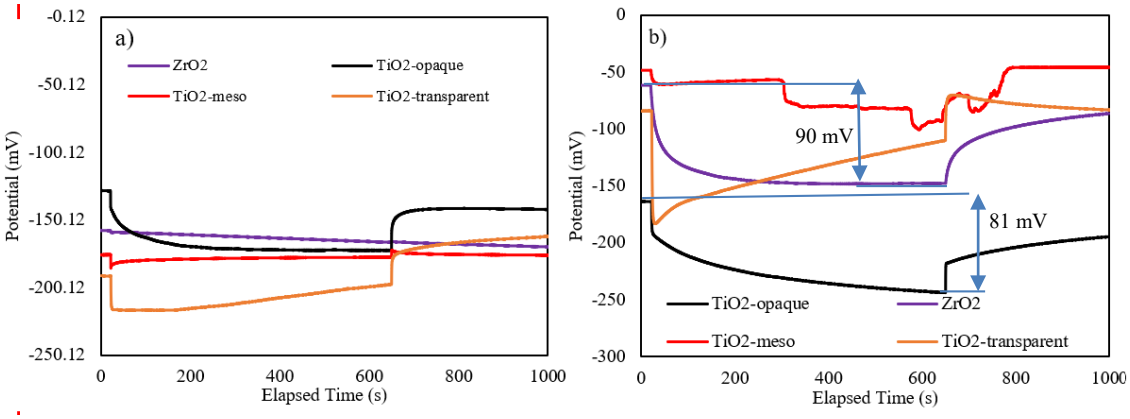

Figure 4: Open circuit voltage results of the hybrid devices with different anodes a) first day and b) after one week.

In order to assess the photocurrent generation capabilities of the devices, a test was conducted by subjecting each device to a short circuit with light pulses. As illustrated in Figure 5, all the devices exhibited the ability to generate photocurrents. It is noteworthy that the current was not zero even prior to the devices being exposed to light. This occurrence can be attributed to the storage capacity of the hybrid cells, enabling the accumulated charges to supply power to an external load even in the absence of light.

Again, the device with the ZrO_2 coating had no photovoltaic response when it was fresh, but after one week it presented about 0.5 µA photocurrent. Almost the same as that in the opaque TiO_2. However, the current was showing a significant offset on the TiO_2 device, due to the stored charges.

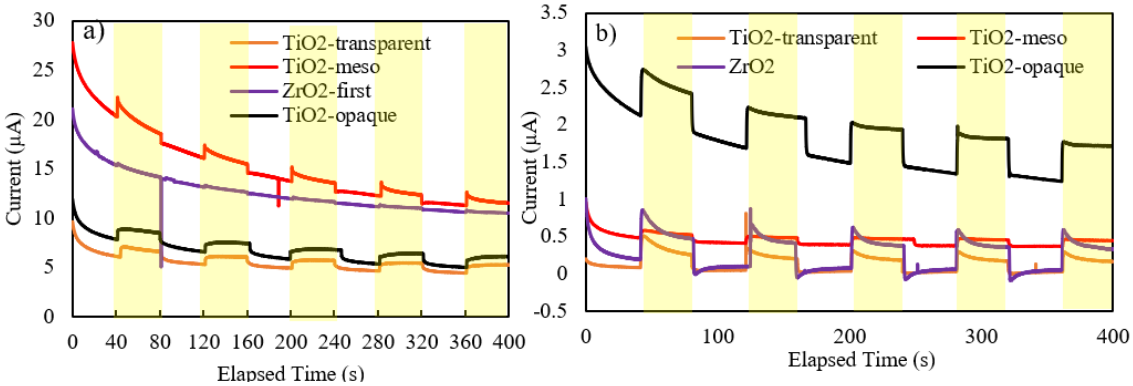

Fig.5: Short circuit current results of the hybrid device with different anodes a) first day and b) after one week.

4. CONCLUSION

In this investigation, four distinct devices were examined, namely transparent- TiO_2, mesoporous- TiO_2, opaque- TiO_2, and TiO_2coated with a thin layer of ZrO_2. The primary objective was to identify the most optimal energy storage and photovoltaic performance among these devices for a two-terminal hybrid system. Both transparent and opaque- TiO_2 exhibited promising outcomes since fresh day. However, noteworthy advancements were observed in the performance of TiO_2 coated with ZrO_2 after a week, indicating a significant enhancement in its energy storage and photovoltaic capabilities. Evidently, ZrO_2 has the potential to enhance the stability of TiO_2 and concurrently mitigate the recombination rate of collected charges within the device. Consequently, this leads to a notable enhancement in both capacitance and photovoltaic characteristics of TiO_2.

ACKNOWLEDGEMENT

This work was supported by a grant from National Science Foundation (NSF 1953089).

REFERENCES

[1] R. Amirabad, A. Ramazani Saadatabadi, M. Pourjahanbakhsh, and M. H. Siadati, "Enhancing Seebeck coefficient and electrical conductivity of polyaniline/carbon nanotube–coated thermoelectric fabric," *Journal of Industrial Textiles,* vol. 51, no. 2_suppl, pp. 3297S-3308S, 2022.

[2] R. Amirabad, A. Ramazani Saadatabadi, and M. H. Siadati, "Preparation of polyaniline/graphene coated wearable thermoelectric fabric using ultrasonic-assisted dip-coating method," *Materials for Renewable and Sustainable Energy,* vol. 9, pp. 1-12, 2020.

[3] A. Takshi, B. Aljafari, T. Kareri *et al.*, "A Critical Review on the Voltage Requirement in Hybrid Cells with Solar Energy Harvesting and Energy Storage Capability," Batteries & Supercaps, 4(2), 252-267 (2021).

[4] A. A. Kamel, H. Rezk, and M. A. Abdelkareem, "Enhancing the operation of fuel cell-photovoltaic-battery-supercapacitor renewable system through a hybrid energy management strategy," *International Journal of Hydrogen Energy,* vol. 46, no. 8, pp. 6061-6075, 2021.

[5] J. Xu, Y. Chen, and L. Dai, "Efficiently photo-charging lithium-ion battery by perovskite solar cell," *Nature communications,* vol. 6, no. 1, p. 8103, 2015.

[6] A. Takshi, H. Yaghoubi, T. Tevi, and S. Bakhshi, "Photoactive supercapacitors for solar energy harvesting and storage," *Journal of Power Sources,* vol. 275, pp. 621-626, 2015.

[7] B. Aljafari, M. K. Ram, and A. Takshi, "Integrated electrochemical energy storage and photovoltaic device with a gel electrolyte," in *Physics, Simulation, and Photonic Engineering of Photovoltaic Devices VIII*, 2019, vol. 10913: SPIE, pp. 145-151.

[8] T. Kareri, B. Aljafari, and A. Takshi, "Hybrid photovoltaic-supercapacitors: effect of the counter electrode on the device performance," in *New Concepts in Solar and Thermal Radiation Conversion IV*, 2021, vol. 11824: SPIE, pp. 22-27.
[9] T. Kareri, M. S. Hossain, M. K. Ram, and A. Takshi, "A flexible fiber-shaped hybrid cell with a photoactive gel electrolyte for concurrent solar energy harvesting and charge storage," *International Journal of Energy Research,* vol. 46, no. 12, pp. 17084-17095, 2022.
[10] Aljafari B, Indrakar SK, Ram MK, Biswas PK, Stefanakos E, Takshi A. A Polyaniline-Based Redox-Active Composite Gel Electrolyte with Photo-Electric and Electrochromic Properties. ChemElectroChem. 2019 Dec 2;6(23):5888-95.
[11] K. Kierzek, E. Frackowiak, G. Lota, G. Gryglewicz, and J. Machnikowski, "Electrochemical capacitors based on highly porous carbons prepared by KOH activation," *Electrochimica Acta,* vol. 49, no. 4, pp. 515-523, 2004.
[12] M. D. Stoller and R. S. Ruoff, "Best practice methods for determining an electrode material's performance for ultracapacitors," *Energy & Environmental Science,* vol. 3, no. 9, pp. 1294-1301, 2010.
[13] S. Zhang and N. Pan, "Supercapacitors performance evaluation," *Advanced Energy Materials,* vol. 5, no. 6, p. 1401401, 2015.
[14] T. Kareri, R. L. Yadav, and A. Takshi, "Image processing analysis of supercapacitors with twisted fiber structures and a gel electrolyte," *Journal of Applied Electrochemistry,* vol. 52, pp. 139-148, 2022.